Available online at www.sciencedirect.com
ScienceDirect
Journal of Colloid and Interface Science 307 (2007) 229–234
JOURNAL OF Colloid and Interface Science
www.elsevier.com/locate/jcis

Effect of hydrogen-bonding interactions on the self-assembly formation of sodium *N*-(11-acrylamidoundecanoyl)-L-serinate, L-asparaginate, and L-glutaminate in aqueous solution

Sumita Roy, Joykrishna Dey *

Department of Chemistry, Indian Institute of Technology, Kharagpur-721 302, India

Received 24 September 2006; accepted 9 November 2006

Available online 11 November 2006

Abstract

Aggregation behavior of three *N*-acyl amino acid surfactants, sodium *N*-(11-acrylamidoundecanoyl)-L-serinate (SAUS), sodium *N*-(11-acrylamidoundecanoyl)-L-asparaginate (SAUAS), and sodium *N*-(11-acrylamidoundecanoyl)-L-glutaminate (SAUGL), was studied in aqueous solution by use of surface tension, fluorescence, dynamic light scattering, and transmission electron microscopic techniques. The amphiphiles have been shown to initially form flexible bilayer structures, which upon increase of surfactant concentration transform into closed spherical vesicles. The transmission electron micrographs of the aqueous solutions of the surfactants confirmed the existence of spherical vesicles. Dynamic light scattering measurements were performed to obtain hydrodynamic radii of the vesicles. Circular dichroism spectra of the amphiphiles indicated formation of chiral helical aggregates in the case of SAUS. The self-assembly formation of the amphiphiles has been discussed in light of the intermolecular hydrogen bonding interaction of the amide groups.

Keywords: *N*-acyl amino acids; Vesicle; Fluorescence; Light scattering; Circular dichroism; Microscopy

1. Introduction

It is well established that the morphology of aggregates formed by amphiphiles is affected by the change in the headgroup structure and hydrocarbon tail. In fact, the possible driving force for the formation of helical and/or cylindrical aggregates is the interaction between headgroups of the amphiphiles [1–6]. Recent studies have shown that short-range attractive interactions such as hydrogen bonding could also be a driving force in the formation of bilayer self-assemblies [7–13]. More recently, we have shown that intermolecular hydrogen bonding between secondary amide groups in the hydrophobic tail of sodium 11-acrylamidoundecanoate (SAU) [7] induces a stable linear state. Others have also reported intermolecular hydrogen-bonding (HB) interaction of the amide group bonded to chiral carbon of *N*-acyl amino acid (NAA) surfactants in Langmuir–Blodgett (LB) monolayers [9,14]. Effects of variation of the structure of the surfactant headgroup of NAA surfactants on the self-assembly properties and microstructure formation have not been studied in detail, although such a structural modification produces some interesting consequences [8–13]. Miyagishi et al. have studied the aggregation behavior of a series of NAA surfactants in water [15,16]. They derived a relationship between the surface activity of an NAA surfactant and the hydrophobicity of the amino acid side chain [16]. Recently, we have investigated the aggregation behavior of sodium *N*-(11-acrylamidoundecanoyl)-L-valinate (SAUV), and L-threoninate (SAUT) in water [17]. The intermolecular amide HB between hydrophobic chains was shown to be responsible for bilayer formation. It was observed that the presence of –OH group in the amino acid side chain of SAUT lowered the critical aggregation concentration (cac) for bilayer structure formation.

The present study is a part of our interest in effects of the structure of the surfactant headgroup on the self-assembly properties and microstructure formation of chiral surfactants. In order to further shed light on the role of hydrogen-bonding functional group in the amino acid side chain of the surfactant head-

* Corresponding author. Fax: +91 3222 255303.
E-mail address: joydey@chem.iitkgp.ernet.in (J. Dey).

0021-9797/$ – see front matter
doi:10.1016/j.jcis.2006.11.014

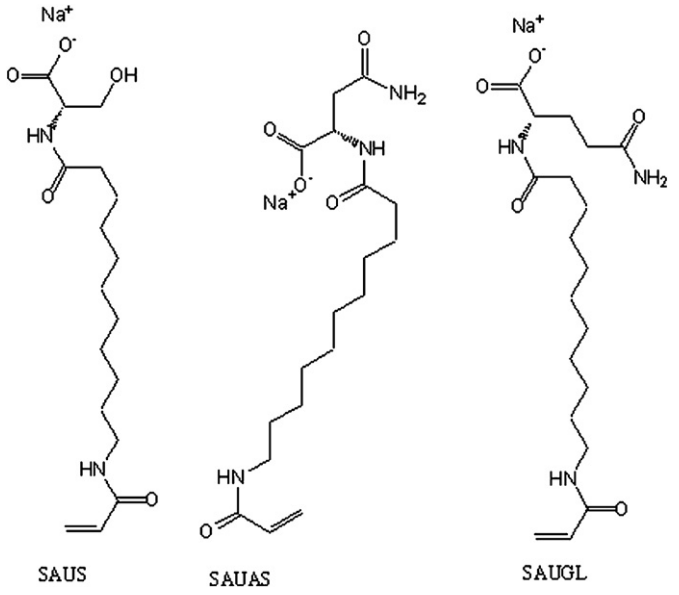

Chart 1. Molecular structures of SAUS, SAUAS, and SAUGL.

group on the self-assembly properties, three NAA surfactants, sodium *N*-(11-acrylamidoundecanoyl)-L-serinate (SAUS), L-asparaginate (SAUAS), and L-glutaminate (SAUGL), were synthesized. The hydrophilic headgroups of these amphiphiles are simple optically active α-amino acids. Earlier studies demonstrated the role of secondary amide bond linked to the surfactant headgroup in the formation of vesicular aggregates of SAUA [8]. The primary amide group of the amino acid side chain in SAUAS and SAUGL can also participate in either intramolecular or intermolecular HB interaction and thereby can influence the self-organization characteristics of the amphiphiles. The molecular structures (see Chart 1) of the amphiphiles show that there can be formation of three stable intermolecular hydrogen bonds. Therefore, the primary objective is to study the effect of the primary amide group in the amino acid side chain in SAUAS and SAUGL amphiphiles on their self-assembly formation. The aggregation behavior of these surfactants has been compared with those of SAUA [8] and SAUV [17], which have no HB site in the amino acid side chain. The microstructures of the self-assemblies in solution were studied to examine if chiral self-assemblies are formed by the surfactants. The mean size of the self-assemblies has been determined.

2. Materials and methods

The fluorescence probes pyrene, and 1,6-diphenyl-1,3,5-hexatriene, DPH (Aldrich) were recrystallized from acetone–ethanol mixture at least three times. Purity of the compounds was tested by the fluorescence emission and excitation spectra. Acryloyl chloride (Aldrich) and 11-aminoundecanoic acid (Aldrich), *N*-hydroxysuccinimide, dicyclohexyl-carbodiimide, L-serine, L-asparagine, and L-glutamine which were procured from SRL and were used without further purification. The salts, acids and bases were all analytical grade and procured locally. All solvents used were of good quality commercially available and whenever necessary were purified, dried and distilled fresh before use. Sodium salts of *N*-(11-acrylamidoundecanoyl)-L-serine, L-asparagine, and L-glutamine were synthesized and purified according to the procedure described in our earlier paper [8,17]. The chemical structures of the compounds were confirmed by elemental analysis, ^{1}H NMR, and FT-IR spectra.

The ^{1}H NMR spectra were recorded on a Bruker SEM 200 instrument in $CDCl_3$ solvent using TMS as standard. The UV–visible spectra were recorded in a Shimadzu (model 1601) spectrophotometer. FT-IR spectra of all the compounds were recorded in a Thermo Nicolet Nexus 870 spectrometer. The circular dichroism (CD) spectra were recorded on a Jasco J-810 spectropolarimeter using quartz cell of 1, 2 or 10 mm path length. The optical rotation was measured with a Jasco P-1020 digital polarimeter. The pH measurements were done with a digital pH meter Model pH 5652 (EC India Ltd., Calcutta) using a glass electrode. All measurements were carried out at room temperature ($\sim$30 °C) unless otherwise mentioned.

The surface tension measurements were performed at room temperature ($\sim$30 °C) with a Torsion Balance (Hardson & Co., Kolkata) using Du Nüoy ring detachment method. The glassware was cleaned thoroughly in sulfochromic acid overnight and then carefully washed with distilled water. The Pt–Ir ring was thoroughly cleaned with 50% ethanol–HCl mixture, rinsed with distilled water and then flamed before each experiment. The surface tension of pure water (71.18 mN m^{-1} at 30 °C) was regularly checked. A stock solution of surfactant was made using Milli-Q water (18.2 M Ω). Aliquot of this solution was transferred to a beaker containing known volume water. The solution was gently stirred magnetically and allowed to stand for about 5 min at room temperature ($\sim$30 °C) and then surface tension was measured. Measurements were repeated at least 3 times and accepted whenever the results did not differ by more than 0.1 mN m^{-1}.

The steady-state fluorescence spectra were measured on a SPEX Fluorolog-3 (model FL3-11) spectrophotometer in the "S/R" mode using 1-nm bandpass for both excitation and emission monochromators. A saturated solution of pyrene in Milli-Q water was used for sample preparation. The pyrene solutions were excited at 335 nm and emission intensity was measured in the wavelength range of 350–550 nm. The average spectrum of at least three runs was recorded. Each spectrum was blank subtracted and was corrected for wavelength dependence of lamp intensity. Steady-state fluorescence anisotropy (r) was measured on a Perkin Elmer LS-55 luminescence spectrometer equipped with filter polarizers that uses the L-format configuration. The temperature of the water-jacketed cell holder was controlled by use of a Thermo Neslab (RTE 7) circulating bath. Since DPH is insoluble in water, a 1.0 mM stock solution of the probe in 20% (v/v) methanol–water mixture was prepared. The final concentration of the probe was adjusted to 2 μM by addition of an appropriate amount of the stock solution. The sample was excited at 350 nm and the emission intensity was followed at 450 nm. The excitation and emission slits widths were respectively, 2.5 and 5 nm. The emission was detected through a cutoff filter for wavelengths below 430 nm. The r-value was

calculated from

$$r = (I_{VV} - GI_{VH})/(I_{VV} + 2GI_{VH}), \quad (1)$$

where I_{VV} and I_{VH} are the fluorescence intensities polarized parallel and perpendicular to the excitation light, G is the instrumental grating factor ($G = I_{HV}/I_{HH}$).

The size of aggregates was determined by dynamic light scattering (DLS) with a Photal DLS-7000 (Otsuka Electronics CO. Ltd., Osaka, Japan) light scattering instrument using 75 mW argon ion laser at a wavelength of 488 nm. The scattering intensity was measured in the angular range 30°–135°. The data acquisition was carried out for 10 min and each experiment was repeated two or three times. Surfactant solutions were prepared with Milli-Q water. The solution was filtered through a Millipore Millex syringe filter (0.22 μm) directly into the scattering cell. Prior to the measurements, the scattering cell was rinsed several times with the filtered solution. The DLS measurements started 5–10 min after the sample solutions were placed in the DLS optical system to allow the sample to equilibrate at the bath temperature. For all light scattering measurements, the temperature was 25 ± 0.5 °C. To analyze the autocorrelation function, the method of cumulant was used [18].

Transmission electron microscopy (TEM) measurements were performed using a 5 mM solution of the amphiphiles after equilibration for 2–3 h. A carbon-coated copper grid was immersed in a drop of aqueous solution of the amphiphile for 1 min, blotted with filter paper, and negatively stained with freshly prepared 1.0% aqueous uranyl acetate. The specimens were air-dried for an hour and then examined on a Phillips CM 200 Electron Microscope operating at an accelerating voltage of 200 kV at room temperature.

3. Results and discussion

3.1. Critical aggregation concentration

Critical aggregation concentration (cac) of the amphiphiles was determined by surface tension (γ) measurements. The plots of γ vs $\log C$ for the aqueous solutions (pH 8) of the amphiphiles are presented in Fig. 1. The surface tension isotherm of all the three amphiphiles exhibits two breakpoints. Similar behavior was also observed with the corresponding glycine (SAUG) and L-valine (SAUV) derivatives in which the first breakpoint was attributed to the formation of flat lamellar structures whereas the second was ascribed to the transformation of lamellar structure to spherical vesicles [8,17]. One can also argue that the first break might be due to formation of pre-micellar aggregates at lower concentrations. The possibility of formation of pre-micellar aggregates can be ruled out, as such structure formation does not normally exhibit break in the surface tension plot. However, this has been eliminated based on the results of fluorescence probe studies using DPH as a probe molecule discussed below.

Since SAUS, SAUAS, and SAUGL are structurally similar, the aggregation behavior is also expected to be similar. Thus the concentrations corresponding to the first and second break in the surface tension isotherm were referred to as cac and cvc

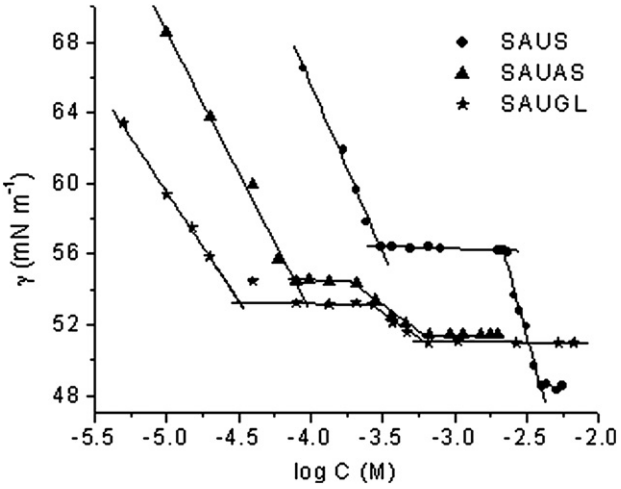

Fig. 1. Plot of γ vs $\log C$ of SAUS, SAUAS, and SAUGL.

Table 1
Self-assembly properties of SAUS, SAUAS, and SAUGL in aqueous solutions at 30 °C

Properties	SAUS	SAUAS	SAUGL
cac (mM)	0.31, 0.45[a]	0.08, 0.04[a]	0.03, 0.02[a]
cvc (mM)	4.03, 3.99[a]	0.61, 0.59[a]	0.62, 0.41[a]
R_h (nm)[b]	74.6	39.0	73.6
I_1/I_3[c]	1.66, 1.48	1.62, 1.46	1.65, 1.44
r	0.140	0.214	0.186
η_m (mPa s)[d]	61.72	138.67	93.38

[a] Data obtained from fluorescence probe studies.
[b] Measurement was done at 25 °C.
[c] First value corresponds to cac, and the second one to cvc.
[d] Data taken from Ref. [26].

(critical vesicle concentration), respectively. The cac and cvc values of the amphiphiles are listed in Table 1. The lower values of cac and cvc suggest that aggregation is more favored in the cases of SAUAS and SAUGL. It is well known that hydrogen-bonding (HB) interaction between the secondary amide groups of adjacent NAA surfactant molecules facilitates aggregate formation [6,19–25]. The relatively stronger intermolecular HB interaction between the primary ($CONH_2$) and the secondary (CONH) amide groups of adjacent surfactant molecules might be responsible for lowering the cac of SAUAS and SAUGL compared to that of SAUS.

3.2. Size of the aggregates

The mean hydrodynamic radius of the aggregates formed was therefore determined by DLS measurements. The apparent translational diffusion coefficient (D) of the aggregates was obtained from the slope of the plot of relaxation rate, Γ ($= Dq^2$) versus square of scattering vector (q) (figure not shown). The plots are linear and pass through origin suggesting that the apparent diffusion coefficient is due to Brownian motion of the particles. The average hydrodynamic radius (R_h) of the particles was calculated using the Stokes–Einstein equation for spherical particles. The average R_h values of the aggregates formed by the amphiphiles in 5 mM solution are listed in

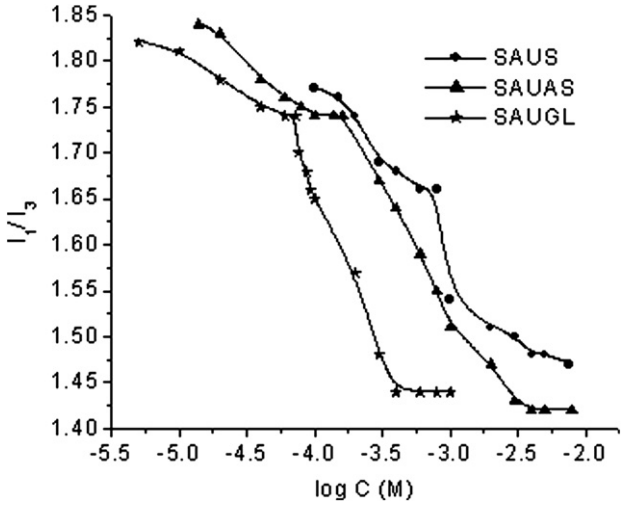

Fig. 2. Plot of polarity ratio I_1/I_3 versus log C of SAUS, SAUAS, and SAUGL.

Table 1. The R_h values thus obtained are very large compared to that of normal spherical micelles, the size for which is usually less than 5 nm. Bilayer vesicles and rod-like micelles have usually large sizes compared to that of normal micelles. The results of DLS studies therefore indicate formation of vesicular and/or rod-like microstructures in aqueous solutions of the amphiphiles.

3.3. Fluorescence probe studies

In order to investigate the nature of self-assemblies at concentrations around cac of the amphiphiles, steady-state fluorescence spectra of pyrene probe were recorded. The representative plots of the ratio of the intensities of the first and third vibronic peaks (I_1/I_3) as a function of surfactant concentration are shown in Fig. 2. A clear two-step change of I_1/I_3 value with the increase in surfactant concentration is evident from the plots. This is consistent with the two breaks in the surface tension plots (Fig. 1). The cac and cvc values (Table 1) thus obtained from the inflection points are found to be closely similar to the values obtained from surface tension measurements. The polarity ratios for both types of aggregates of all the amphiphiles are indicated in Table 1. The low I_1/I_3 values of pyrene fluorescence compared to that in water (1.83) indicate solubilization of the probe in hydrophobic environment. However, the relatively large value of I_1/I_3 ratio below cvc compared to that of spherical micelles suggests that the self-assemblies have flat structures such as bilayer membranes.

Fluorescence anisotropy of DPH probe was also measured at various concentrations above the cac in order to determine the microenvironment of the aggregate. The anisotropy (see Table 1) value is relatively high at concentrations above the first transition, which remained unchanged with the increase of surfactant concentration even above cvc. The r-values in 5 mM surfactant solutions are listed in Table 1. The high value of r suggests an ordered environment around the DPH probe in the self-assemblies. In a recent publication [26], we have shown that microviscosity (η_m) in the self-assemblies formed by these surfactants is very high compared to that of micellar aggregates. The relatively large value of r and hence η_m suggested existence of bilayer aggregates. This excludes formation of any pre-micellar aggregates. The high r-value below cvc could also be explained if bicelles or disk-like micelles were formed. However, since bicelles have closed structures, the I_1/I_3 ratio is expected to be like micellar aggregates. Moreover, bicelles are usually formed in mixed micellar systems in which one of the amphiphiles assembles into bilayer structures and the other forms micellar aggregates. Therefore, the possibility of formation of disk-like micelles in the case of pure SAUS, SAUAS, and SAUGL amphiphiles can be ruled out. Thus high micropolarity and high η_m values below cvc suggest formation of flat bilayer structures.

We have already shown that bilayer aggregates of SAUG and SAUA are formed as a result of intermolecular HB interaction between the secondary amide groups at the end of the hydrocarbon tail and near the surfactant head group of neighboring molecules [8]. Similar hydrogen bond formation is also expected in the bilayer aggregates of SAUS, SAUAS, and SAUGL surfactants. However, participation of the primary amide group of the amino acid side chain in SAUAS and SAUGL in intermolecular HB interaction with neighboring molecules cannot be overlooked. The lower values of cac in the cases of SAUAS and SAUGL compared to that of SAUS may be due to this stronger intermolecular HB interaction between primary amide group of the amino acid side chain and the secondary amide group linked to the headgroup of another molecule in the bilayer assembly. This enhances the hydrophobic interaction between hydrocarbon chains leading to tight packing, which is reflected in the high r-values of DPH probe in the self-assemblies of SAUAS and SAUGL compared to that of SAUS.

3.4. Transmission electron microscopy

To investigate the microstructure of the self-assemblies of SAUS, SAUAS, and SAUGL, TEM pictures were taken in aqueous solution. No identifiable structures could be seen under microscope when surfactant solutions had concentrations less than cvc value. The TEM images of 5 mM aqueous solutions of SAUS, SAUAS, and SAUGL are shown in Figs. 3A–3F. The micrographs for SAUS exhibit spherical vesicles that were spontaneously formed in solution. In addition to the vesicles, the presence of closed tubule is also observed in aqueous solution of SAUS (Fig. 3B). It appears that the tubules are formed by the fusion of the vesicles. The vesicles of SAUS have internal diameter in the range of 80–210 nm. The micrographs of SAUAS (Figs. 3C and 3D) and of SAUGL (Figs. 3E and 3F) exhibit two types of morphologies including small as well as large spherical vesicles (Figs. 3C, 3E and 3F) and tubules (Fig. 3D). The vesicles of SAUAS have inner diameter in the range of 70–280 nm. The hollow tubule is closed at two ends and has a length 9 μm and channel width of 900 nm. Most probably these are formed through fusion of smaller spherical vesicles. On the other hand, the large spherical vesicles as well as elliptical vesicles of SAUGL (Figs. 3E and 3F) have diameter in the range 200 nm to 2 μm. Since the micrographs were obtained from the same samples, it suggests that all the structures that

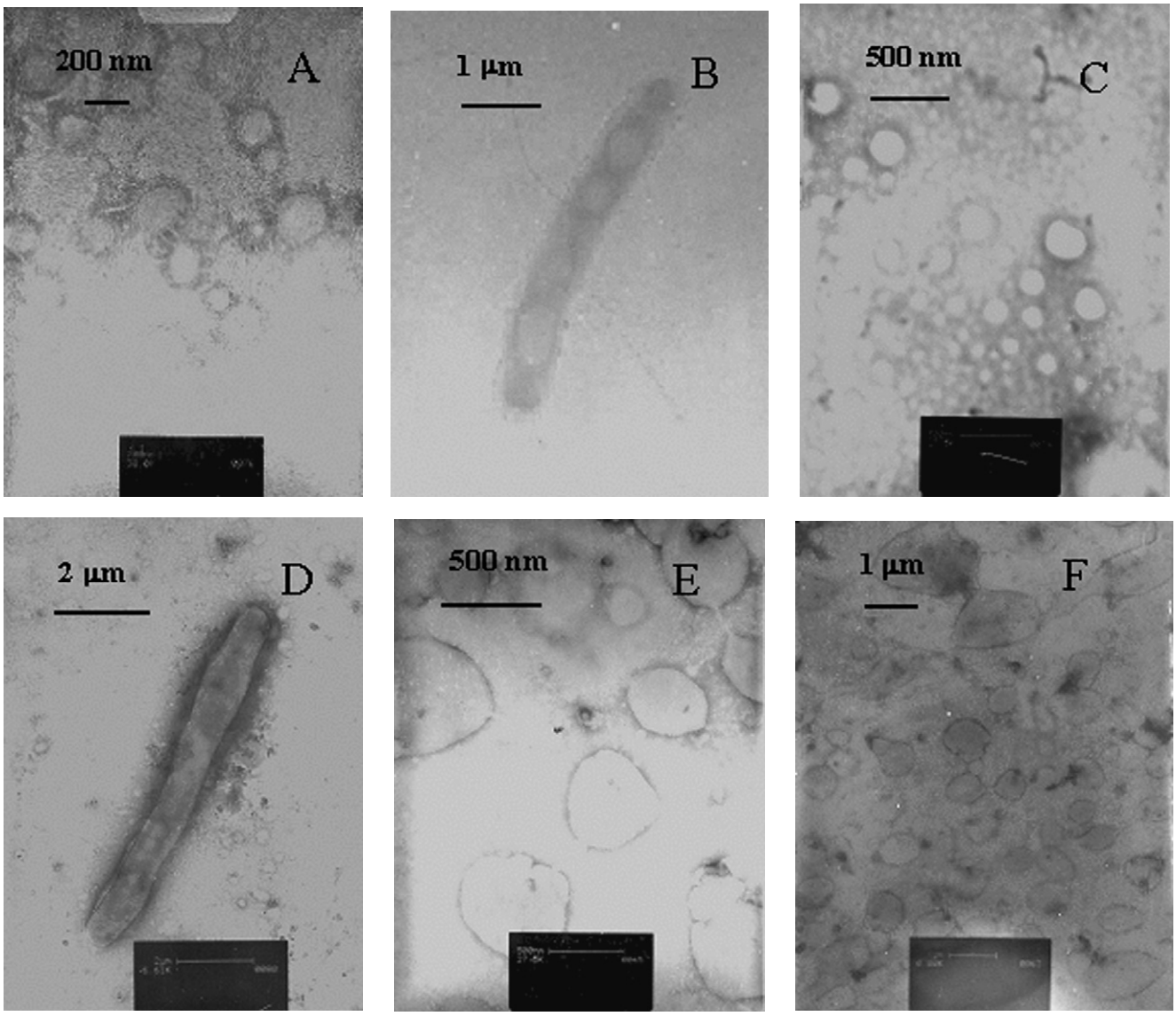

Fig. 3. Transmission electron micrographs of 5 mM aqueous solution of SAUS (A, B), SAUAS (C, D), and SAUGL (E, F).

coexist were spontaneously formed in solution. The size of the vesicles obtained from TEM pictures are much larger than that obtained from DLS measurements as the latter method gives only the average value.

3.5. Circular dichroism spectra

The CD spectra recorded in aqueous solutions of the amphiphiles at concentrations above and below the respective cac are shown in Fig. 4. The CD spectra have similarity with those of SAUA, SAUV and SAUT [8,17]. The CD band with $\lambda_{max} \sim 212$ nm can be attributed to the $\pi \rightarrow \pi^*$ transition of the amide carbonyl group [27–29]. At concentrations below cac, the peak at 212 nm disappears and a new peak at 200 nm appears. The disappearance of the CD band at 212 nm below cac indicates formation of chiral structures through aggregation. It is important to note that the molar ellipticity of the 212-nm band is very low in the CD spectra of SAUAS and SAUGL surfactants suggesting that the tendency to form chiral aggregates is very weak. It has been shown by others [19,21, 23,30] as well as by us [7,8,17] that intermolecular HB interaction between secondary amide groups is responsible for the formation of chiral helical aggregates of the NAA surfactant. In the case of SAUAS and SAUGL, perhaps the intermolecular HB interaction between secondary amide groups is weakened due to the relatively stronger hydrogen bond formation between the primary $CONH_2$ group of the amino acid side chain of the surfactant headgroup with the secondary CONH group of an adjacent molecule in the same layer.

4. Concluding remarks

The sodium *N*-(11-acrylamidoundecanoyl)-L-serinate, L-asparaginate, and L-glutaminate undergo self-assembly formation in two steps with two cac values. The lower cac is associated with the formation of planar bilayer aggregates and the higher

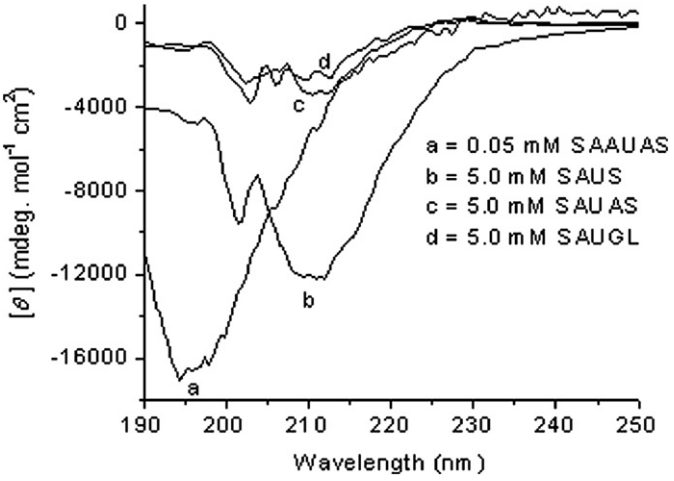

Fig. 4. CD spectra of SAUS, SAUAS, and SAUGL in water.

one corresponds to formation of closed vesicles. The low values of cac are due to intermolecular hydrogen bonding interactions between amide groups. The low values of the first cac of SAUAS and SAUGL as compared to SAUS are due to the hydrogen bonding capability of the $CONH_2$ group at the amino acid side chain of the amphiphiles. While intermolecular amide hydrogen bonding between hydrophobic tails is responsible for the formation of flat bilayer structures the amide hydrogen bonding near the surfactant headgroup is the driving force for secondary aggregation. The intermolecular amide hydrogen bonding interaction between $CONH_2$ group at the amino acid side chain with the secondary amide group (CONH) of neighboring molecule inhibits formation of chiral aggregates, which is manifested by the low molar ellipticity of the CD band in the cases of SAUAS and SAUGL.

Acknowledgment

Financial support for this work came from CSIR (Grant No. 01(2008)/05/EMR-II).

References

[1] H. Hidaka, M. Murata, T. Onai, J. Chem. Soc. Chem. Commun. (1984) 562.
[2] N. Ramanathan, A.L. Currie, J.R. Colvin, Nature 190 (1961) 779.
[3] N. Nakashima, S. Asakuma, J.-M. Kim, T. Kunitake, Chem. Lett. (1984) 1709.
[4] J.-H. Fuhrhop, P. Schnieder, J. Rosenberg, E. Boekema, J. Am. Chem. Soc. 109 (1987) 3387.
[5] J.-H. Fuhrhop, P. Schnieder, E. Boekema, W. Helfrich, J. Am. Chem. Soc. 110 (1988) 2861.
[6] J.-H. Fuhrhop, C. Demoulin, J. Rosenberg, C. Boettcher, J. Am. Chem. Soc. 112 (1990) 2827.
[7] S. Roy, J. Dey, Langmuir 19 (2003) 9625.
[8] S. Roy, J. Dey, Langmuir 21 (2005) 10362.
[9] H. Maeda, R. Kakehashi, Adv. Colloid Interface Sci. 88 (2000) 275.
[10] H. Kawasaki, H. Maeda, Langmuir 17 (2001) 2278.
[11] B.S. Li, J. Chen, C.F. Zhu, K.K.L. Leung, L. Wan, C. Bai, B.Z. Tang, Langmuir 20 (2004) 2515.
[12] D. Kaneko, U. Olsson, K. Sakamoto, Langmuir 18 (2002) 4699.
[13] S. Bhattacharya, Y. Krishnan-Ghosh, J. Chem. Soc. Chem. Commun. (2001) 185.
[14] X. Du, Y. Liang, Langmuir 16 (2000) 3422.
[15] S. Miyagishi, S. Matsumura, K. Murata, T. Asakawa, M. Nishida, Bull. Chem. Soc. Jpn. 58 (1985) 1019.
[16] S. Miyagishi, T. Asakawa, M. Nishida, J. Colloid Interface Sci. 131 (1989) 68.
[17] S. Roy, J. Dey, Bull. Chem. Soc. Jpn. 79 (2006) 1.
[18] D.E. Koppel, J. Chem. Phys. 57 (1972) 4814.
[19] M. Shinitzky, R. Haimovitz, J. Am. Chem. Soc. 115 (1993) 12545.
[20] Y.-J. Zhang, M. Jin, R. Lu, Y. Song, L. Jiang, Y. Zhao, J. Phys. Chem. B 106 (2002) 1960.
[21] C. Boettcher, B. Schade, J.-H. Fuhrhop, Langmuir 17 (2001) 873.
[22] J.-H. Fuhrhop, P. Schnieder, J. Rosenberg, E. Boekema, J. Am. Chem. Soc. 109 (1989) 3387.
[23] T. Imae, Y. Takahashi, H. Muramatsu, J. Am. Chem. Soc. 114 (1992) 3414.
[24] D. Vollhardt, U. Gehlert, J. Phys. Chem. B 106 (2002) 4419.
[25] H. Kawasaki, M. Souda, S. Tanaka, N. Nemoto, G. Karlsson, M. Almgren, H. Maeda, J. Phys. Chem. B 106 (2002) 1524.
[26] S. Roy, A. Mohanty, J. Dey, Chem. Phys. Lett. 414 (2005) 23.
[27] W. Moffitt, J. Chem. Phys. 25 (1956) 467.
[28] W.B. Gratzer, G.M. Holtzwarth, P. Doty, Proc. Natl. Acad. Sci. USA 47 (1961) 1785.
[29] K. Rosenheck, B. Sommer, J. Chem. Phys. 46 (1967) 532.
[30] S. Borocci, G. Mancini, G. Cerichelli, L. Luchetti, Langmuir 15 (1999) 2627.